

## Rhabdomyosarcoma: Molecular analysis of *Igf2*, *MyoD1* and *Myogenin* expression.

L. KRŠKOVA<sup>1</sup>, A. AUGUSTINAKOVA<sup>1</sup>, E. DRAHOKOUPILOVA<sup>2</sup>, D. SUMERAUER<sup>2</sup>, P. MUDRY<sup>3</sup>, R. KODET<sup>1</sup>

<sup>1</sup>Department of Pathology and Molecular Medicine, 2<sup>nd</sup> Faculty of Medicine, Charles University and Faculty Hospital in Motol, Prague, Czech Republic, e-mail: lkrskova@email.cz; <sup>2</sup>Department of Pediatric Hematology and Oncology, 2<sup>nd</sup> Faculty of Medicine, Charles University and Faculty Hospital in Motol, Prague, Czech Republic; <sup>3</sup>Clinic of Pediatric Oncology, Faculty Hospital in Brno

Received January 23, 2011

Rhabdomyosarcoma is the most common soft tissue sarcoma of childhood. There are two major histopathological types of RMS – embryonal (eRMS) and alveolar (aRMS). A molecular study of *Igf2*, *MyoD1* and *Myogenin* was performed to determine the expression profiles and to assess the possible utility of these genes as potential treatment targets. Patients with RMS showed up to 100-fold increase of *Igf2* transcription in comparison with normal skeletal muscle. Our data suggest that overexpression of *Igf2* occurs in RMS of both histological subtypes. No correlation between the results of *Igf2* mRNA expression and LOH at the 11p15 region ( $p=0.12$ ) was observed, but there was a trend of a higher expression of *Igf2* mRNA in RMS samples with LOH.

We observed a high level of *MyoD1* mRNA in both aRMS and eRMS, and we detected a similar level of *MyoD1* mRNA in RMS and normal skeletal muscles. There was a correlation between the results of *MyoD1* mRNA expression and LOH at the 11p15 region.

We did not observe any statistical difference in the level of *Myogenin* mRNA in the subgroups of RMS. Analogous to *MyoD1*, we observed a similar level of *Myogenin* mRNA in RMS and normal skeletal muscles.

*Key words:* Rhabdomyosarcoma; Real-time RT-PCR; *Igf2*, *MyoD1*, *Myogenin*, Loss of heterozygosity

Rhabdomyosarcoma (RMS) is the most common soft tissue sarcoma of childhood. The tumor accounts for approximately two thirds of all sarcomas of children aged 0 – 14 years, and approximately for 8 % of malignant solid tumors in childhood [1].

RMS is of mesenchymal origin and may arise virtually anywhere in the body. Its diagnosis is based on identification of rhabdomyoblastic differentiation of tumor cells. There are two major histopathological types of RMS commonly seen in pediatric practice – embryonal (eRMS) and alveolar (aRMS). In 60 to 70 % of aRMS one of two characteristic chromosomal translocations are found: t(2;13)(q35;q14) involving *PAX3* gene at 2q and *FKHR* gene at 13q or a variant translocation t(1;13)(q36;p14) which fuses *PAX7* gene with *FKHR* [2]. These translocations result in an alteration of biological activity at protein level and are thought to influence tumorigenic behavior having impact on control of the tumor cell growth, apoptosis, differentiation and motility [3]. No primary molecular genetic aberration analogous to the *FKHR* rearrangement has been detected in eRMS. A high

frequency of loss of heterozygosity (LOH) at a chromosomal region 11p15, a region known to contain several imprinted genes including insulin-like growth factor 2 (*Igf2*), *H19* and *p57<sup>KIP2</sup>*, has been found in eRMS [4], but other studies have shown that both eRMS and aRMS are associated with LOH and loss of imprinting (LOI) of genes mapping to 11p15 [5]. Moreover, alteration of the imprinting of the *Igf2* gene has been published in Wilm's tumor, and RMS with retention of heterozygosity (ROH) in 11p15 were identified [6,7,8]. These findings support a notion that maternal-specific LOH and LOI of *Igf2* are alternative pathways contributing to tumorigenesis through the up-regulation of IGF2.

Insulin-like growth factor 2 (IGF2) has been shown to play an important role in the development, growth, and survival of normal cells. IGF2 is encoded by the imprinted *Igf2* gene expressed only from the paternal allele in most tissues [8]. Overexpression of *Igf2* has been observed in several types of sporadic human neoplasms and this phenomenon has been attributed to loss of imprinting of the maternal allele [9,10]. Consequently, LOI of *Igf2* has been proposed as an important

mechanism of tumorigenesis. Overexpression of *Igf2* may be caused also by uniparental disomy involving duplication of the paternal (non-imprinted) locus, and loss of the maternal (imprinted) locus [9]. Alternatively, increased *Igf2* transcription could reflect amplification of the *Igf2* gene in the tumor or *Igf2* might become a target of abnormally activated signaling pathways. For example, Khan et al found that *PAX3-FKHR* in aRMS but not *PAX3* alone is able to activate a number of genes, including *Igf2* and activates myogenic transcriptional program including induction of *MyoD1* transcription, *Myogenin* and *Six1* as well as a number of other muscle-specific genes [11]. A role of IGF2 in myogenic differentiation has been demonstrated by identifying this peptide as an autocrine differentiation factor in myoblasts [12] as well as a survival factor during the transition from proliferating to differentiating myoblasts [13]. IGF2 overexpressing myoblasts undergo enhanced differentiation characterized by accelerated expression of *Myogenin* mRNA and extensive myotube formation [14].

The basic helix-loop-helix transcription factors of the MyoD family (*MyoD*, *myf-5*, *Myogenin*, *MRF4*) play a central role in myogenesis [15]. Many studies have demonstrated that these proteins individually can convert uncommitted mesenchymal precursors to the myoblastic lineage [16]. *MyoD* and *myf-5* are essential for myoblast specification during early embryonic development [17], *Myogenin* is critical for the cell differentiation [18] and *MRF4* plays a secondary role in muscle formation [19].

The myogenic determination (*MyoD*) gene was first identified by virtue of its ability to convert nonmuscle cells into muscle cells [20]. *Myogenin* gene is a direct transcriptional target of *MyoD* [15]. Activation of *Myogenin* gene transcription occurs as a very early event in *MyoD*-regulated muscle differentiation, and it is preceded by the accumulation of key regulatory proteins, including *MyoD* at the proximal *Myogenin* promoter.

The study of Wilson and Rotwein shows that inhibition of *Igf2* expression in differentiating myoblasts blocked reversibly *MyoD*-mediated muscle differentiation [15]. Blockade of this

pathway inhibits stimulation of *Myogenin* gene expression, and prevents morphological differentiation. The absence of IGF2 signaling did not change the abundance of *MyoD1* in the nucleus or at the *Myogenin* promoter.

To investigate the potential importance of IGF2 in pathogenesis of RMS of both alveolar and embryonal subtypes we analyzed tumor material and correlated histotype with the presence of characteristic translocations and expression status of *Igf2*, *MyoD1* and *Myogenin*, as well as LOH of 11p15.

## Materials and methods

**Sample collection and patients samples.** There were 35 boys and 35 girls in the study group. Histologically, 42 patients were diagnosed with alveolar and 28 with embryonal RMS. Twenty six patients with alveolar RMS had chimeric products identified (21 *PAX3-FKHR* and 5 *PAX7-FKHR*). 16 cases with alveolar morphology were fusion gene negative aRMS – Table 1a. Eleven patients with aRMS had favorable localization of the primary tumor and 31 had unfavorable primary sites (parameningeal, extremity and genitourinary – bladder or prostate). Similarly, 13 patients with eRMS had favorable and 15 unfavorable localizations of tumors. Samples of bone marrow or peripheral blood progenitor cells were collected in EDTA at the time of the tumor diagnosis and, in some cases, during chemotherapy. The tumors were diagnosed by light microscopy using hematoxylin and eosin staining complemented by immunohistochemistry. A panel of primary antibodies included vimentin (dilution 1:100, DAKO – clone V97), desmin (dilution 1:100, DAKO – clone D33), sarcomeric actin (dilution 1:75, DAKO – clone Alpha-Sr-1), *MyoD1* protein (dilution 1:50, DAKO – clone 5.8A), *myogenin* (dilution 1:30, DAKO – clone F5D) and anti CD99 (dilution 1:500, Lab Vision – clone O13).

To determine the specificity of *Igf2*, *MyoD1* and *Myogenin* for RMS at the molecular level we analyzed a group of neoplasms other than RMS – Table 1b.

**RNA extraction and preparation of complementary DNA (cDNA).** RNA was extracted from 10 x 5µm thick sections

Table 1a

RMS samples	fusion gene	<i>Igf2<sub>N</sub></i> median mean value	<i>MyoD1<sub>N</sub></i> median mean value	<i>Myogenin<sub>N</sub></i> median mean value
42 aRMS	21 <i>PAX3/FKHR</i> +	1.92 x 10 <sup>9</sup>	1.45 x 10 <sup>5</sup>	7.51 x 10 <sup>6</sup>
		6.13 x 10 <sup>9</sup>	5.04 x 10 <sup>5</sup>	2.29 x 10 <sup>7</sup>
	5 <i>PAX7/FKHR</i> +	1.77 x 10 <sup>9</sup>	1.95 x 10 <sup>5</sup>	6.63 x 10 <sup>5</sup>
		2.12 x 10 <sup>9</sup>	1.84 x 10 <sup>5</sup>	1.21 x 10 <sup>6</sup>
	16 <i>PAX3-7/FKHR</i> -	1.1 x 10 <sup>9</sup>	2.89 x 10 <sup>5</sup>	2.3 x 10 <sup>6</sup>
28 eRMS	28 <i>PAX3-7/FKHR</i> -	3.0 x 10 <sup>9</sup>	6.02 x 10 <sup>5</sup>	3.84 x 10 <sup>6</sup>
		1.64 x 10 <sup>9</sup>	1.85 x 10 <sup>5</sup>	9.75 x 10 <sup>5</sup>
		1.77 x 10 <sup>10</sup>	5.6 x 10 <sup>5</sup>	5.71 x 10 <sup>6</sup>

Patient's data and results of the study

*Igf2<sub>N</sub>* RQ- absolute quantification of *Igf2* mRNA; *MyoD1<sub>N</sub>* RQ- absolute quantification of *MyoD1* mRNA; *Myogenin<sub>N</sub>* RQ- absolute quantification of *Myogenin* mRNA.

Table 1b Non-RMS samples

Type	Number	<i>Igf2</i> <sub>N</sub> median mean value	<i>MyoD1</i> <sub>N</sub> median mean value	<i>Myogenin</i> <sub>N</sub> median mean value
BM from healthy donors	6	1.55 x 10 <sup>3</sup> 1.94 x 10 <sup>4</sup>	0.0 x 10 <sup>0</sup> 1.93 x 10 <sup>0</sup>	2.91 x 10 <sup>1</sup> 1.62 x 10 <sup>1</sup>
Adult muscle	6	4.1 x 10 <sup>7</sup> 1.78 x 10 <sup>8</sup>	1.64 x 10 <sup>5</sup> 1.90 x 10 <sup>5</sup>	7.2 x 10 <sup>6</sup> 6.97 x 10 <sup>6</sup>
Non-RMS tumors	16	5.67 x 10 <sup>5</sup> 1.87 x 10 <sup>8</sup>	5.49 x 10 <sup>5</sup> 7.9 x 10 <sup>5</sup>	1.43 x 10 <sup>3</sup> 2.27 x 10 <sup>5</sup>
teratoma	1			
EWS	1			
alveolar sarcoma of soft tissues	1			
infantile fibromatosis	2			
infantile fibrosarcoma	1			
leiomyocellular sarcoma	3			
leiomyoma	3			
epitheloid sarcoma	1			
rhabdoid tumors	2			
hemangiopericytoma	1			
Non-Hodgkin lymphomas	6	2.62 x 10 <sup>5</sup> 1.85 x 10 <sup>6</sup>	2.74 x 10 <sup>0</sup> 7.51 x 10 <sup>0</sup>	1.54 x 10 <sup>1</sup> 1.72 x 10 <sup>2</sup>
mucosa assoc. lymph. tissue lymph.	2			
mantle cell lymphoma	4			
Ductal breast carcinoma	10	2.15 x 10 <sup>5</sup> 3.48 x 10 <sup>5</sup>	0.0 x 10 <sup>0</sup> 7.51 x 10 <sup>0</sup>	3.07 x 10 <sup>1</sup> 5.29 x 10 <sup>1</sup>

Patient's data and results of the study

*Igf2*<sub>N</sub> RQ- absolute quantification of *Igf2* mRNA; *MyoD1*<sub>N</sub> RQ- absolute quantification of *MyoD1* mRNA; *Myogenin*<sub>N</sub> RQ- absolute quantification of *Myogenin* mRNA.

of the tumor tissue or from bone marrow samples using Tri-Reagent (Invitrogen Corporation, Carlsbad, CA) according to the manufacturer's instructions.

Forty four samples obtained from various non-neoplastic tissues or neoplasms were extracted using the same protocol (Table 1b).

Complementary DNA was prepared from 1 µl of RNA in 20 µl of reaction volume. The protocol was described by Krsková et al [21].

Quantitative RT-PCR for fusion gene *PAX3-7/FKHR*, *Igf2*, *Myogenin* and for *MyoD1* was performed on LightCycler (Roche), using TaqMan technology. Primers and probes are listed in the Table 2. *PAX3/FKHR* and *PAX7/FKHR* primers and probes for RQ-RT-PCR were designed by TipMolBiol, *MyoD1* primers and probe was obtained from Applied Biosystems. For the *Myogenin* and *Igf2* gene expression measurement, we applied RQ-RT-PCR with LNA probe generated by means of the Universal Probe Library for Human found at the website [www.universalprobelibrary.com](http://www.universalprobelibrary.com) (Roche, Mannheim, Germany). Human *Beta 2 microglobulin* (*β2M*) was used as a housekeeping gene [22]. Amplifications of both fusion transcripts and *MyoD1* were under identical PCR conditions on LightCycler. cDNA was amplified with a mix consisting of: Platinum Taq Polymerase 1 U in the PCR buffer provided by the manufac-

turer (Gibco BRL), 4.5 mM MgCl<sub>2</sub>, 0.2 mM each dNTP, 0.25 µg/µl BSA, 0.5 µM of each primer, 0.2 µM of hydrolyzation probe, 1 µl of cDNA in a final volume of 20 µl. The reaction mixture was subjected to denaturation at 95 °C for 90s followed by 50 cycles of rapid amplification – denaturation at 95 °C for 10s, annealing at 60 °C for 35s on LightCycler (Roche, Mannheim, Germany).

Amplification of *Myogenin* was under the following PCR conditions on LightCycler. The PCR mix was composed of Platinum Taq DNA Polymerase (1 unit in the PCR buffer provided by the manufacturer, Gibco BRL, Carlsbad, Tex); MgCl<sub>2</sub> (3.5 mM), dNTPs (0.2 mM each); BSA (0.25 µg/µl); primers (0.2 µM each); probe (0.1 µM) and cDNA (1 µl) in a final volume of 20 µl. The program consisted of incubation at 40 °C for 2 minutes and initial denaturation at 95 °C for 2 minutes, followed by 45 cycles at 95 °C for 10 sec., and 60 °C for 35 sec (single fluorescence measurement).

For *Igf2* expression measurement we applied single-round RQ-RT-PCR in SYBR Green format with primers described by Zhan et al [7] (sequences in the Table 2). The mix for *Igf2* quantification was as follows: Platinum Taq DNA Polymerase (1 unit in the PCR buffer provided by the manufacturer, Gibco BRL, Carlsbad, Tex); MgCl<sub>2</sub> (4.5 mM), dNTPs (0.2 mM each); BSA (0.25 µg/µl); primers (0.5 µM each); 2µl of 5x10<sup>-4</sup> SYBR

**Table 2. List of primers**

<i>β2-microglobulin</i>	
<i>β2M-F</i>	5' TGA CTT TGT CAC AGC CCA AGA TA - 3'
<i>β2M-R</i>	5' AAT CCA AAT GCG GCA TCT TC - 3'
<i>β2M Probe</i>	5' TGA TGC TGC TTA CAT GTC TCG ATC CCA - 3'
MyoD1 (mix of primers and probe obtained from Applied Biosystem)	
Igf2	
Igf2-F	5' CTT GGA CTT TGA GTC AAA TTG G - 3'
Igf2-R	5' GGT CGT GCC AAT TAC ATT TCA - 3'
SybrGreen	
PAX3/FKHR	
PAX3-S	5' CCC CAT GAA CCC CAC CA - 3'
FKHR-A	5' GAA TGA ACT TGC TGT GTA GGG ACA 3'
PAX3/FKHR probe	5' TGG CCT CTC ACC TCA GAA TTC AAT TCG T 3'
PAX7/FKHR	
PAX7-F	5' GCG CCC TCC AAC CAC AT - 3'
FKHR-A	5' GAA TGA ACT TGC TGT GTA GGG ACA 3'
PAX7/FKHR probe	5' ACG GCC TGT CTC CTC AGA ATT CAQA TTC GT 3'
Myogenin-F	5' CAG CTC CCT CAA CCA GGA G 3'
Myogenin-R	5' GCT GTG AGA GCT GCA TTC G 3'
LNA probe No 20	

List of primers and probes

Green (FMC BioProducts, Rockland, MA, USA) and cDNA (1 μl) in a final volume of 20 μl. The program consisted of the initial denaturation step at 95 °C for 2 minutes, followed by 50 cycles at 95 °C for 15 sec., and 60 °C for 35 sec, 72 °C for 15 sec (single fluorescence measurement). The melting curve analysis consisted of the following steps: 95 °C for 15 sec., 55 °C for 10 sec and then heating to 95 °C with continual measurement of fluorescence.

***β2-microglobulin* and PAX3/7-FKHR, MyoD1 plasmid DNA calibrators.** The *β2-microglobulin*, fusion genes, *Myogenin*, *Igf2* and *MyoD1* sequences were cloned into a PCR 2.1 TOPO cloning vector and were transformed into *E. coli* recipient culture, using the TOPO TA Cloning Kit (Invitrogen). The selected clones were screened using Miniprep method and quantified using spectrophotometer.

**Normalization of *β2-microglobulin* and fuse genes, Myogenin, Igf2 or MyoD1 expression.** The expression of all genes was calculated using absolute quantification. Plasmids with the insert were diluted in decimal steps into Salmon Sperm DNA. A diluting line of plasmids was used for preparation of standard curves. Normalized expression (*MyoD1<sub>N</sub>*, *Myogenin<sub>N</sub>*, *Igf2<sub>N</sub>* or *PAX3/7-FKHR<sub>N</sub>*) was determined as a ratio between gene transcript and *β2-microglobulin* levels.

Each PCR run was performed in duplicate and the mean value of results was calculated.

**Table 3. List of STR markers**

D11S1363 A:	6-Fam-	GAA AAT GGT ATT TAG AAA CCA A
D11S1363 B		CCC AAG GGC TTA CAA C
THO A:	6- Fam-	GTG GGC TGA AAA GCT CCC GAT TAT
THO B		ATT CAA AGG GTA TCT GGG CTC TGG
D11S1338 A:	6- Fam-	GAC GGT TTA ACT GTA TAT CTA AGA C
D11S1338 B:		TAA TGC TAC TTA TTT GGA GTG TG
D11S921 A:	6-Fam-	TGC ATT CAA CAA
D11S921 B		CTT GGA CCA TTT ATT CTA AAG TAA T
D11S1307 A	6-Fam-	TTT GTG TTG TGG CAG ACA CT
D11S1307 B		AGA GGC CAG CCT GTG TG
D11S1888 A	6-Fam-	CCC CAG TAC CCT GTA TAG GC
D11S1888 B		CAC TTG TGT GTT TGT ATC GAG TCA

Primers from LOH study

**LOH study.** The presence of LOH was studied in 42 patients' samples obtained from the tumors at the time of diagnosis, or from recurrent lesions. Each sample was compared with constitutional DNA of the same patient obtained from bone marrow aspirate or from peripheral blood. All constitutional samples were without tumor cell contamination as confirmed by molecular techniques (negative results of RT-PCR for MyoD1, α/γ acetylcholine receptor, PAX3/FKHR and PAX7/FKHR).

**Polymorphic STR markers.** A panel of 6 highly informative microsatellite markers was used. Table 3 shows a list of these markers.

Amplification was performed with primers labeled with fluorescent dye (6-FAM) in a final volume 20 μl containing 50 – 100 ng of DNA template, 1-2 mM MgCl<sub>2</sub>, 10 pM of each primer, 0.2 mM dNTPs, 1 x reaction buffer, and 0.3 U Taq polymerase (Top-Bio, Prague, Czech Republic). Amplification was performed in an automated thermal cycler with 5 min 95 °C denaturation step followed by 30 cycles of 94 °C denaturation 30 sec, annealing at the temperature 60 – 66 °C for 45 sec, and extension at 72 °C 30 sec. The last cycle was followed by a final extension at 72 °C for 20 min. PCR products were detected by fragment analysis using an automated genetic analyzer ABI PRISM 310 (Applied Biosystems, Foster City, California, USA).

**Statistical analysis.** We used the JMP IN 5.1 software (SAS Institute, Cary, NC, USA). To establish whether mRNA differences were significant a non-parametric one-way analysis of variance, the Kruskal-Wallis or Mann-Whitney tests were utilized. RQ-RT-PCR correlations were measured with Spearman's coefficient of correlation. For all tests, *p* < 0.05 was considered significant.

## Results

**LOH study.** We screened 42 paired tumor / peripheral blood or bone marrow samples without tumor cell contamination for LOH from 14 patients with eRMS and 28 patients with

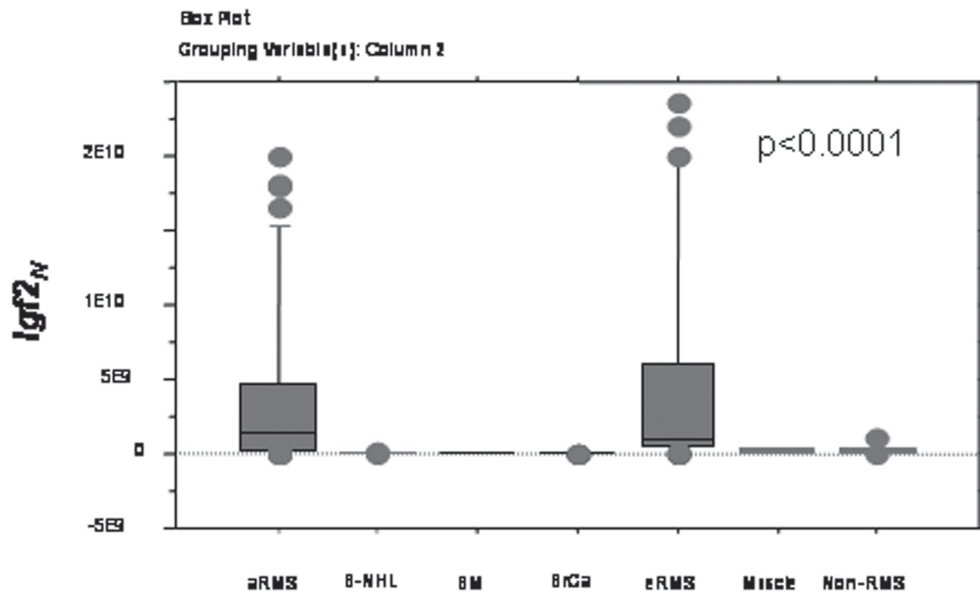


Figure 1. Box plot graph demonstrates the distribution of *Igf2<sub>N</sub>* levels among groups of different tumors and tissues. Subgroups of patients with aRMS and eRMS expressed a significantly higher levels than all other subgroups (Man-Whitney;  $p < 0.0001$ ). Boxes represent values between 25<sup>th</sup> and 75<sup>th</sup> percentile with the median, whiskers represent 10<sup>th</sup> and 90<sup>th</sup> percentile and outlying values are represented by dots.

aRMS. 11/14 informative eRMS patients, 10/22 informative fusion positive aRMS patients and 5/6 informative fusion negative aRMS patients demonstrated LOH at least in one of the microsatellite loci in the region 11p15.

The frequency of LOH on 11p from telomere to 11p14 was as follows: D11S1363 54,5% – THO 50% – D11S1338 37,5% – D11S1307 54% – D11S921 42% – D11S1888 27% in patients with aRMSs, and D11S1363 100% – TH 67% – D11S1338 67% – D11S1307 43% – D11S921 25% – D11S1888 57% in patients with eRMSs. The last three microsatellite markers (D11S1307, D11S921, D11S1888) from the region 11p15 map close to the *MyoD1* gene, which is a regulatory factor of muscle differentiation and a molecular marker of RMS. The frequency of LOH in this region was surprisingly high, which suggests that this region of LOH includes the *MyoD1* locus.

**The level of *Igf2* mRNA in RMS.** We did not observe any statistical difference in the level of *Igf2<sub>N</sub>* mRNA in the two subgroups of RMS. The median of *Igf2<sub>N</sub>* mRNA for PAX3-FKHR positive aRMS was  $1.92 \times 10^9$ , mean value  $6.13 \times 10^9$ ; the median of *Igf2<sub>N</sub>* mRNA for PAX7-FKHR positive aRMS was  $1.77 \times 10^9$ , mean value  $2.12 \times 10^9$ ; the median of *Igf2<sub>N</sub>* mRNA for fusion-negative aRMS was  $1.11 \times 10^9$ , mean value  $3 \times 10^9$ . For eRMS the median value was  $1.64 \times 10^9$ , mean  $1.77 \times 10^{10}$ .

A statistical analysis of different control tumors (Tab. 1b) using the nonparametric Kruskal-Wallis test showed significantly different mRNA level of *Igf2* between RMS and the control group of tumors ( $p < 0.0001$ ) – Fig 1. Additionally, we showed 100-fold higher level of *Igf2* mRNA in RMS than in muscle specimens (median value was  $4.1 \times 10^7$ , mean  $1.78 \times 10^8$ ).

We observed a high level of *Igf2* mRNA in both aRMS and eRMS ( $p = 0.54$ ) and in both *PAX/FKHR* fusion products ( $p = 0.58$ ). No correlation was observed between the results of *Igf2* mRNA expression and age ( $p = 0.48$ ), sex ( $p = 0.43$ ), metastases ( $p = 0.86$ ), relapse of the disease ( $p = 0.23$ ). The correlation was observed between the results of *Igf2* mRNA expression and localization of the primary tumor – favorable or unfavorable ( $p = 0.011$ ). No correlation was observed between the results of *Igf2* mRNA expression and LOH at the region ( $p = 0.12$ ).

**The level of *MyoD1* mRNA in RMS.** We did not observe any statistical difference in the level of *MyoD1<sub>N</sub>* mRNA in subgroups of RMS. The median of *MyoD1<sub>N</sub>* mRNA for fusion-positive aRMS was  $1.17 \times 10^5$ , mean value  $3.29 \times 10^5$ ; the median of *MyoD1<sub>N</sub>* mRNA for fusion-negative aRMS was  $2.89 \times 10^5$ , mean value  $6.02 \times 10^5$ , and for eRMS the median value was  $1.85 \times 10^5$ , mean  $5.6 \times 10^5$ . We observed a very similar level of *MyoD1* mRNA in RMS and normal skeletal muscles (median value was  $1.64 \times 10^5$ , mean  $1.9 \times 10^5$ ).

We observed a high level of *MyoD1* mRNA in both *PAX/FKHR* fusion products ( $p = 0.72$ ). The relation between age and generalization of the disease at diagnosis (the two principal risk factors of RMS) and *MyoD1* expression in the primary tumor samples was analyzed. In children at different age groups no major difference in *MyoD1* expression was observed ( $p > 0.05$ ). A similar finding was observed for groups of localized and metastatic RMSs ( $p = 0.31$ ). No correlations were observed between the results of *MyoD1* mRNA expression and sex ( $p = 0.53$ ), localization of the primary tumor – favorable or unfavorable ( $p = 0.25$ ), relapse of the disease ( $p = 0.39$ ) and survival ( $p = 0.65$ ). The correlation was observed between the

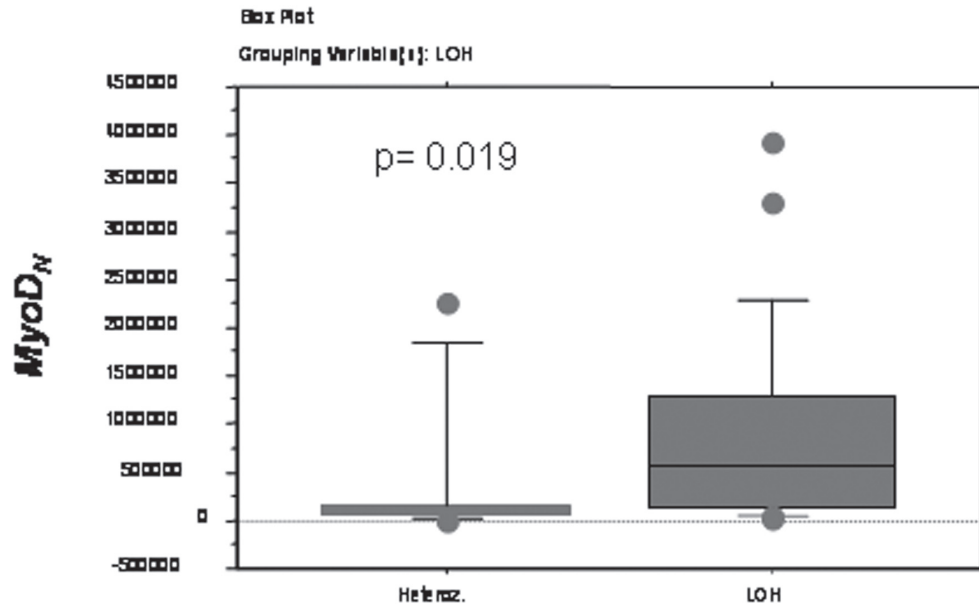


Figure 2. MyoD1 expression in RMS in relation to heterozygosity or LOH at the region 11p15 (Kruskal – Wallis;  $p = 0.019$ ).

results of *MyoD1* mRNA expression and LOH at the 11p15 region ( $p = 0.019$ ) – Fig.2. The high level of *MyoD1* mRNA correlated with *Igf2* mRNA level ( $p = 0.003$ ).

**The level of Myogenin mRNA in RMS.** We did not observe any statistical difference in the level of *Myogenin<sub>N</sub>* mRNA in subgroups of RMS. The median of *Myogenin<sub>N</sub>* mRNA for PAX3-FKHR positive aRMS was  $7.512 \times 10^5$ , mean value  $2.29 \times 10^7$ ; the median of *Myogenin<sub>N</sub>* mRNA for PAX7-FKHR positive aRMS was  $6.63 \times 10^5$ , mean value  $1.21 \times 10^6$ , the median of *Myogenin<sub>N</sub>* mRNA for fusion-negative aRMS was  $2.3 \times 10^6$ , mean value  $3.84 \times 10^6$ , and for eRMS the median value was  $9.75 \times 10^5$ , mean  $5.71 \times 10^6$ . We observed a similar level of *Myogenin* mRNA in RMS and normal skeletal muscles (median value was  $7.2 \times 10^6$ , mean  $6.97 \times 10^6$ ).

We observed a high level of *Myogenin* mRNA in both aRMS and eRMS ( $p = 0.17$ ) and a higher level in RMS with PAX3/FKHR fusion product than in PAX7/FKHR fusion product ( $p = 0.027$ ). No correlations were observed between the results of *Myogenin* mRNA expression and age ( $p = 0.32$ ), sex ( $p = 0.60$ ), and relapse of the disease ( $p = 0.13$ ). We observed a trend of a higher level of *Myogenin* mRNA as compared with localization of the primary tumor – favorable or unfavorable ( $p = 0.064$ ), and a generalized disease at the time of presentation ( $p = 0.068$ ) and a relapse ( $p = 0.18$ ). No correlation was observed between the results of *Myogenin* mRNA expression and LOH at the 11p15 region ( $p = 0.56$ ).

The high level of *Myogenin* mRNA correlated with *Igf2* mRNA level ( $p = 0.008$ ) and *MyoD* mRNA level ( $p < 0.0001$ ).

**Specificity of PAX3/7-FKHR fusion gene for aRMS.** PAX3-FKHR or PAX7-FKHR transcripts were found specific for aRMS. We did not find PAX3/7-FKHR positivity in any

of non-RMS tumors. The median of *PAX3-FKHR<sub>N</sub>* mRNA for aRMS was  $1.18 \times 10^5$ , mean value  $6.11 \times 10^5$ , and median of *PAX7-FKHR<sub>N</sub>* mRNA for aRMS was  $2.75 \times 10^3$ , mean value  $6.26 \times 10^3$ .

## Discussion

Genomic imprinting is the preferential way of silencing one parental allele due to epigenetic modifications. Insulin-like growth factor 2 (*Igf2*), which codes for a potent mitogen [23, 24], is an imprinted gene located at chromosome 11p15.5 in human. In most tissues *Igf2* is maternally imprinted. Loss of *Igf2* imprinting commonly occurs in various tumors, and it may be involved in malignant transformation [25,26]. *Igf2* loss of imprinting leads to biallelic production of IGF2 protein. IGF2 is an important fetal growth stimulatory factor and it is involved in RAS-RAF-MAPK cascade and in the PI3 cascade whose activation results in both cell cycle progression and protection from apoptosis.

IGF2 appears to be important for growth of osteosarcoma; suppression of IGF2 in osteosarcoma cell lines leads to growth inhibition [27]. Similarly, our results point out to an important role of *Igf2* overexpression in the pathogenesis of RMS. Because IGF2 is indispensable for tumor transformation of RMS, we aimed to determine the mechanism involved in *Igf2* overexpression. *Igf2* transcripts were quantified using TaqMan assay. Patients with RMS showed up to 100-fold increase of *Igf2* transcription in comparison with normal skeletal muscle. Our data suggest that overexpression of *Igf2* occurs in RMS of both histological subtypes and both in the absence or in the presence of the tumor specific translocations. Possible mecha-

nisms of *Igf2* overexpression could rest in uniparental disomy, polyploidy or in loss of imprinting. Increased IGF2 expression could also reflect amplification of the *Igf2* gene in the tumor or, alternatively, *Igf2* may become a target of an abnormally activated PTCH signaling pathway [28]. Uniparental disomy is caused by a loss of the maternal (imprinted) *Igf2* locus with a concomitant duplication of the paternal *Igf2* locus. In our study no correlation was observed between the results of *Igf2* mRNA expression and LOH at the 11p15 region ( $p=0.12$ ), but with a trend of a higher expression of *Igf2* mRNA in RMS samples with LOH at the 11p15.5 region. These data provided support for the potential role of LOH with uniparental disomy in overexpression of *Igf2* in a significant proportion of our RMS patients. The findings of Minniti et al. show that unregulated overexpression of IGF2 growth factor interferes with myogenic differentiation as defined by a lack of myotube formation and a decrease in the expression of *Myogenin* [29]. In our study we found a 100-fold higher level of *Igf2* mRNA in patients with RMS than in non-neoplastic muscle specimens, but a very similar level of *MyoD1* and *Myogenin* mRNAs in both RMS and normal muscles.

Khan et al. found that PAX3-FKHR but not PAX3 alone was able to activate a number of genes, including *Igf2* [11]. We observed a high level of *Igf2* mRNA in both aRMS and eRMS ( $p=0.54$ ) and in both PAX/FKHR fusion products ( $p=0.58$ ). We can, therefore, speculate that *Igf2* gene is not a candidate downstream target of PAX3-FKHR pathway in aRMS.

A high percentage of LOH was identified on chromosome 11p. These results suggest the presence of either a cluster of tumor suppressor genes or a single pleiotropic gene involved in tumorigenesis localized at 11p15. Moreover, the obtained data indicate that the critical region is centered between the loci D11S1363 and D11S1338. Since LOH in 11p15.5 has been demonstrated in eRMS [30,31], our results from LOH study show, that both alveolar and embryonal subtypes of RMS have alterations at this region. Our data also show similar frequency of LOH in eRMS (78.5%) and fusion negative aRMS patients (83 %) in contrast to fusion positive aRMS (45 %). These data are in conclusion with the study of Davicioni et al, who stated that fusion negative aRMS is more similar to eRMS than to fusion positive aRMS [34]. Also array comparative genomic hybridization (aCGH) indicated that the frequency of a number of gains, amplifications and losses is significantly different between fusion positive aRMS and fusion negative aRMS and eRMS [32]. Williamson et al. demonstrated that fusion negative aRMS is not readily distinguishable from eRMS and that the primary influence on the clinical presentation, outcome and molecular biology of RMS is the presence or absence of a fusion gene [32].

We found LOH between the loci D11S1307 and D11D921 where the gene *MyoD1* maps. The frequency of LOH in this region was surprisingly high, which suggests that this common region of LOH includes the *MyoD1* locus. *MyoD1* (myogenic determination) gene codes for a regulatory factor of muscle differentiation and it is considered a molecular marker of RMS

[31,33]. We found a high level of *MyoD1* mRNA in correlation with LOH at the 11p15 region ( $p=0.019$ ) – Fig.2.

Davicioni et al. reported that *MyoD1* is a PAX/FKHR target gene and that it was expressed in a two-fold higher amount in PAX-FKHR transduced embryonal cell line RD compared with vector control [34]. In contrast to this finding, we did not observe any significant difference between expression levels of *MyoD1* in all subgroups of RMS (both the chimeric gene positive and negative).

In accordance with observations published by Gattenloehner et al. we found that *MyoD1* transcript is not entirely specific for RMS [2]. We found *MyoD1* transcripts in a normal skeletal muscle, a result similar to that seen in aRMS and eRMS. Furthermore, other mesenchymal neoplasms used as a control tissue revealed *MyoD1<sub>N</sub>* expression (median  $1.56 \times 10^2$ , mean value  $3.43 \times 10^4$ ). Some non-Hodgkin's lymphomas (NHLs) show also *MyoD1<sub>N</sub>* expression, though weak (median  $5.45 \times 10^0$ , mean value  $1.16 \times 10^1$ ). All these results diminish the usefulness of *MyoD1* as a single molecular marker in molecular diagnosis of RMS.

In this study we may confirm recent observations showing that there are differences between a strong and uniform pattern of Myogenin positivity in alveolar RMSs whereas the pattern in embryonal RMS is more heterogeneous [35,36,37]. In contrast to the results of immunohistochemistry demonstrating the protein, RQ-RT-PCR data did not reveal different levels of *Myogenin* mRNA in aRMSs and eRMSs. We observed a higher level of *Myogenin* in PAX3/FKHR fusion product in comparison with PAX7/FKHR fusion product ( $p=0.027$ ). It could be caused by an increased transcriptional potency of PAX3/FKHR fusion transcript relative to that of PAX7/FKHR, and it may result in the fact that the tumors with the PAX7/FKHR fusion transcript appear to have a more favorable prognosis [38,39]. This result also suggests that high expression of PAX3-FKHR and *Igf2* in fusion positive aRMS patients could synergistically play a role in oncogenesis and tumor progression of aRMS. In this study we demonstrated the trend of a higher level of *Myogenin* mRNA in comparison with localization of the primary tumor – favorable or unfavorable ( $p=0.064$ ), with a generalized disease at the time of presentation ( $p=0.068$ ), and the disease relapse ( $p=0.046$ ). No correlation was observed between the results of *Myogenin* mRNA expression and LOH at the 11p15 region ( $p=0.56$ ). The high level of *Myogenin* mRNA correlated well with *Igf2* mRNA level ( $p=0.008$ ) and *MyoD* mRNA level ( $<0.0001$ ). It is probably caused by the mechanism in which *MyoD1*, and consequently *Myogenin*, are downstream targets of *Igf2* pathway in both aRMS and eRMS.

Our data demonstrate, that *Myogenin* transcript is not entirely specific for RMS. We found *Myogenin* transcripts in a normal skeletal muscle (median  $7.2 \times 10^6$ ), a result similar to that seen in aRMS and eRMS. Furthermore, other mesenchymal neoplasms used as a control tissue revealed *Myogenin<sub>N</sub>* expression (median  $4.93 \times 10^4$ , mean value  $3.28 \times 10^5$ ). Some non-Hodgkin's lymphomas (NHLs) show also *Myogenin<sub>N</sub>* expression, though weak (median  $1.23 \times 10^0$ , mean value

1.15x10<sup>4</sup>). The positivity of *MyoD1* and *Myogenin* in other tumors is difficult to explain. These data could indicate that both *MyoD1* and *Myogenin* may play a role as transcriptional factors not only in myogenesis.

Future studies of aRMS and eRMS should provide a clearer understanding of translocation-dependent or independent pathways for development of aRMS and the nature of the constitutional molecular changes in eRMSs.

Acknowledgement. The study was supported by the Grant GAČR 304/07/0532, MSM 0021620813 and the Research Project of the Ministry of Health MZOFNM2005.

## References

- [1] MCDOWELL HP. Update on childhood rhabdomyosarcoma. *Arch Dis Child*. 2003; 88 (4): 354-7. doi:10.1136/adc.88.4.354
- [2] GATTENLOEHNER S, DOCKHORN-DWORNICZAK B, LEUSCHNER I, VINCENT A, MÜLLER-HERMELINK HK, et al. A Comparison of *MyoD1* and fetal acetylcholine receptor expression in childhood tumors and normal tissue. *Journal of Mol Diagnostics* 1999; 1: 23-31. doi:10.1016/S1525-1578(10)60605-8
- [3] BARR FG. Gene fusions involving PAX and FOX family members in alveolar rhabdomyosarcoma. *Oncogene*. 2001; 20: 5736-46. doi:10.1038/sj.onc.1204599
- [4] ANDERSON J, GORDON A, MCMANUS A, SHIPLEY J, PRITCHARD-JONES K. Disruption of Imprinted Genes at Chromosome Region 11p15.5 in Paediatric Rhabdomyosarcoma. *Neoplasia* 1999; 1 (4): 340-348. doi:10.1038/sj.neo.7900052
- [5] VISSER M, SIJMONS C, BRAS J, ARCECI RJ, GODFRIED M, et al. Allelotype of pediatric rhabdomyosarcoma. *Oncogene* 1997; 15 : 1309-1314 doi:10.1038/sj.onc.1201302
- [6] STEENMAN MJ, RAINIER S, DOBRY CJ, GRUNDY P, HORON IL, et al. Loss of imprinting of *IGF2* is linked to reduced expression and abnormal methylation of *H19* in Wilms' tumour. *Nat Genet*. 1994; 7: 433-9.
- [7] ZHAN S, SHAPIRO DN, HELMAN LJ. Activation of an imprinted allele of the insulin-like growth factor II gene implicated in rhabdomyosarcoma. *J Clin Invest*. 1994; 94: 445-8. doi:10.1172/JCI117344
- [8] ZHANG L, KIM M, CHOI MK, GOEMANS B, YEUNG C, et al. Diminished G1 Checkpoint after  $\gamma$ -Irradiation and Altered Cell Cycle Regulation by Insulin-like Growth Factor II Overexpression. *J Biol Chem*. 1999; 274: 13118-126. doi:10.1074/jbc.274.19.13118
- [9] REIK W, MAHER ER.: Imprinting in clusters: lessons from Beckwith-Wiedemann syndrome. *Trends Genet*. 1997; 13(8): 330-4. doi:10.1016/S0168-9525(97)01200-6
- [10] MIYAKI M. Imprinting and colorectal cancer. *Nat Med*. 1998; 4: 1236-7. doi:10.1038/3214
- [11] KHAN J, BITTNER ML, SAAL LH, TEICHMANN U, AZORSA DO, et al. cDNA microarrays detect activation of a myogenic transcription program by the PAX3-FKHR fusion oncogene. *Proc Natl Acad Sci U S A*. 1999; 96: 13264-9. doi:10.1073/pnas.96.23.13264
- [12] STEWART CE, JAMES PL, FANT ME, ROTWEIN P. Overexpression of insulin-like growth factor-II induces accelerated myoblast differentiation. *J Cell Physiol*. 1996; 169: 23-32. doi:10.1002/(SICI)1097-4652(199610)169:1<23::AID-JCP3>3.0.CO;2-G
- [13] STEWART CE, ROTWEIN P. Insulin-like growth factor-II is an autocrine survival factor for differentiating myoblasts. *J Biol Chem*. 1996; 271: 11330-8. doi:10.1074/jbc.271.19.11330
- [14] PRELLE K, WOBUS AM, KREBS O, BLUM WF, WOLF E. Overexpression of insulin-like growth factor-II in mouse embryonic stem cells promotes myogenic differentiation. *Biochem Biophys Res Commun*. 2000; 277: 631-8. doi:10.1006/bbrc.2000.3737
- [15] WILSON EM, ROTWEIN P. Control of *MyoD* function during initiation of muscle differentiation by an autocrine signaling pathway activated by insulin-like growth factor-II. *J Biol Chem*. 2006; 281: 29962-71. doi:10.1074/jbc.M605445200
- [16] WEINTRAUB H. The *MyoD* family and myogenesis: redundancy, networks, and thresholds. *Cell*. 1993; 75: 1241-4. doi:10.1016/0092-8674(93)90610-3
- [17] RUDNICKI MA, SCHNEGELSBERG PN, STEAD RH, BRAUN T, ARNOLD HH, et al. *MyoD* or *Myf-5* is required for the formation of skeletal muscle. *Cell*. 1993; 75:1351-9. doi:10.1016/0092-8674(93)90621-V
- [18] HASTY P, BRADLEY A, MORRIS JH, EDMONDSON DG, VENUTI JM, et al. Muscle deficiency and neonatal death in mice with a targeted mutation in the myogenin gene. *Nature*. 1993; 364(6437):501-6. doi:10.1038/364501a0
- [19] OLSON EN, ARNOLD HH, RIGBY PW, WOLD BJ. Know your neighbors: three phenotypes in null mutants of the myogenic bHLH gene *MRF4*. *Cell*. 1996; 85:1-4. doi:10.1016/S0092-8674(00)81073-9
- [20] DAVIS RL, WEINTRAUB H, LASSAR AB. Expression of a single transfected cDNA converts fibroblasts to myoblasts. *Cell* 1987; 24; 51: 987-1000.
- [21] KRŠKOVÁ L, MRHALOVÁ M, HILSKÁ I, SUMERAUER D, DRAHOKOUPÍLOVÁ E, et al. Detection and clinical significance of bone marrow involvement in patients with rhabdomyosarcoma. *Virchows Archiv*. 2010; 456: 463-472. doi:10.1007/s00428-010-0913-9
- [22] BIJWAARD KE, AGUILERA NS, MONCZAK Y, TRUDEL M, TAUBENBERGER JK, et al. Quantitative real-time reverse transcription-PCR assay for cyclin D1 expression: utility in the diagnosis of mantle cell lymphoma. *Clin Chem*. 2001 47: 195-201.
- [23] DECHIARA TM, EFSTRATIADIS A, ROBERTSON EJ. A growth-deficiency phenotype in heterozygous mice carrying an insulin-like growth factor II gene disrupted by targeting. *Nature*. 1990; 345(6270): 78-80. doi:10.1038/345078a0
- [24] ULANER GA, VU TH, LI T, HU JF, YAO XM, et al. Loss of imprinting of *IGF2* and *H19* in osteosarcoma is accompanied by reciprocal methylation changes of a CTCF-binding site. *Hum Mol Genet*. 2003; 12: 535-49. doi:10.1093/hmg/ddg034
- [25] OGAWA O, ECCLES MR, SZETO J, MCNOE LA, YUN K, et al. Relaxation of insulin-like growth factor II gene imprint-

- ing implicated in Wilms' tumour. *Nature*. 1993; 362: 749-51. [doi:10.1038/362749a0](https://doi.org/10.1038/362749a0)
- [26] CUI H, HORON IL, OHLSSON R, HAMILTON SR, FEINBERG AP. Loss of imprinting in normal tissue of colorectal cancer patients with microsatellite instability. *Nat Med*. 1998; 4: 1276-80. [doi:10.1038/3260](https://doi.org/10.1038/3260)
- [27] BRACZKOWSKI R, SCHALLY AV, PLONOWSKI A, VARGA JL, GROOT K, et al. Inhibition of proliferation in human MNNG/HOS osteosarcoma and SK-ES-1 Ewing sarcoma cell lines in vitro and in vivo by antagonists of growth hormone-releasing hormone: effects on insulin-like growth factor II. *Cancer*. 2002; 95: 1735-45. [doi:10.1002/cncr.10865](https://doi.org/10.1002/cncr.10865)
- [28] HAHN H, WOJNOWSKI L, SPECHT K, KAPPLER R, CALZADA-WACK J, et al. Patched Target Igf2 is Indispensable for the formation of medulloblastoma and rhabdomyosarcoma. *J Biol Chemistry* 2000; 257: 28341-28344. [doi:10.1074/jbc.C000352200](https://doi.org/10.1074/jbc.C000352200)
- [29] SCRABLE H, CAVENEE W, GHAVIMI F, LOVELL M, MORGAN K, et al. A model for embryonal rhabdomyosarcoma tumorigenesis that involves genome imprinting. *Proc Natl Acad Sci U S A*. 1989; 86: 7480-4. [doi:10.1073/pnas.86.19.7480](https://doi.org/10.1073/pnas.86.19.7480)
- [30] SCRABLE H, WITTE D, SHIMADA H, SEEMAYER T, SHENG WW, et al. Molecular differential pathology of rhabdomyosarcoma. *Genes Chromosomes Cancer*. 1989; 1:23-35. [doi:10.1002/gcc.2870010106](https://doi.org/10.1002/gcc.2870010106)
- [31] MINNITI CP, LUAN D, O'GRADY CH, ROSENFELD RG, OH Y, et al. Insulin-like Growth Factor II Overexpression in Myoblasts Induces Phenotypic Changes Typical of the Malignant Phenotype. *Cell Growth Diff*. 1995; 6: 263-69.
- [32] WILLIAMSON D, MISSIAGLIA E, DEREYNIES A, PIERRON G, THUILLE B, et al. Fusion gene-negative alveolar rhabdomyosarcoma is clinically and molecularly indistinguishable from embryonal rhabdomyosarcoma. *J. Clin. Oncology* 2010; 28: 2151-2158. [doi:10.1200/JCO.2009.26.3814](https://doi.org/10.1200/JCO.2009.26.3814)
- [33] CHEN B, DIAS P, JENKINS JJ 3RD, SAVELL VH, PARHAM DM. Methylation alterations of the MyoD1 upstream region are predictive of subclassification of human rhabdomyosarcomas. *Am Jf Pathology* 1998; 152: 1071-1079
- [34] DAVICIONI E, FINCKENSTEIN FG, SHAHBAZIAN V, BUCKLEY JD, TRICHE TJ, et al. Identification of a PAX-FKHR gene expression signature that defines molecular classes and determines the prognosis of alveolar rhabdomyosarcomas. *Cancer Res* 2006; 66:6936-46. [doi:10.1158/0008-5472.CAN-05-4578](https://doi.org/10.1158/0008-5472.CAN-05-4578)
- [35] DIAS P, CHEN B, DILDAY B, PALMER H, HOSOI H, et al. Strong immunostaining for myogenin in rhabdomyosarcoma is significantly associated with tumors of the alveolar subclass. *Am J Pathol* 2000; 2: 399-408. [doi:10.1016/S0002-9440\(10\)64743-8](https://doi.org/10.1016/S0002-9440(10)64743-8)
- [36] KUMAR S, PERLMAN E, HARRIS CA, RAFFELD M, TSOKOS M. Myogenin is a specific marker for rhabdomyosarcoma: an immunohistochemical study in paraffin-embedded tissues. *Mod Pathol* 2000; 13: 988-93. [doi:10.1038/modpathol.3880179](https://doi.org/10.1038/modpathol.3880179)
- [37] COFFIN,CM, RULON, J, SMITH, L, BRUGGERS C, WHITE FV. Pathologic features of rhabdomyosarcoma before and after treatment: A clinicopathologic and immunohistochemical analysis. *Mod Pathol* 1997; 10: 1175-87
- [38] BARR FG. Molecular genetics and pathogenesis of rhabdomyosarcoma. *J Pediatr Hematol Oncol* 1997; 19:483-91. [doi:10.1097/00043426-199711000-00001](https://doi.org/10.1097/00043426-199711000-00001)
- [39] BARR FG. The role of chimeric paired box transcription factors in the pathogenesis of pediatric rhabdomyosarcoma. *Cancer Res* 1999; 59 (7 Suppl): 1711-15.